

## Extinction and optical depth of contrails

C. Voigt,<sup>1,2</sup> U. Schumann,<sup>1</sup> P. Jessberger,<sup>1</sup> T. Jurkat,<sup>1</sup> A. Petzold,<sup>1</sup> J.-F. Gayet,<sup>3</sup>  
M. Krämer,<sup>4</sup> T. Thornberry,<sup>5</sup> and D. W. Fahey<sup>5</sup>

Received 2 March 2011; revised 2 May 2011; accepted 3 May 2011; published 14 June 2011.

[1] One factor limiting the understanding of the climate impact from contrails and aircraft induced cloud modifications is the accurate determination of their optical depth. To this end, 14 contrails were sampled for 2756 s with instruments onboard the research aircraft Falcon during the CONCERT (CONtrail and Cirrus ExpeRimenT) campaign in November 2008. The young (<10 min old) contrails were produced by 9 commercial aircraft with weights of 47 to 508 t, among them the largest operating passenger aircraft, the Airbus A380. The contrails were observed at temperatures between 214 and 224 K and altitudes between 8.8 and 11.1 km. The measured mean in-contrail relative humidity with respect to ice was  $89 \pm 12\%$ . Six contrails were observed in cloud free air, the others were embedded in thin cirrus clouds. The observed contrails exhibited a mean ice water content of  $2 \text{ mg m}^{-3}$  and had a mean number concentration of  $117 \text{ cm}^{-3}$  and effective radius of  $2.9 \text{ }\mu\text{m}$  assuming asphericle particles with an aspect ratio of 0.5. Probability density functions of the extinction, with a mean (median) of  $1.2$  ( $0.7$ )  $\text{km}^{-1}$ , and of the optical depth  $\tau$ , with a mean (median) of  $0.27$  ( $0.13$ ), are derived from the in situ measurements and are likely representative for young contrails from the present-day commercial aircraft fleet at observation conditions. Radiative transfer estimates using the in-situ measured contrail optical depth lead to a year-2005 estimate of line-shaped contrail radiative forcing of  $15.9 \text{ mWm}^{-2}$  with an uncertainty range of  $11.1$ – $47.7 \text{ mWm}^{-2}$ . **Citation:** Voigt, C., U. Schumann, P. Jessberger, T. Jurkat, A. Petzold, J.-F. Gayet, M. Krämer, T. Thornberry, and D. W. Fahey (2011), Extinction and optical depth of contrails, *Geophys. Res. Lett.*, 38, L11806, doi:10.1029/2011GL047189.

### 1. Introduction

[2] Despite recent progress, the radiative forcing from persistent contrails and aircraft induced cloudiness remains poorly constrained [Intergovernmental Panel on Climate Change (IPCC), 2007; Lee et al., 2009]. Uncertainties lie in understanding of the formation processes of aircraft induced cirrus cloudiness and in the quantification of persistent contrail cover and contrail optical depth [IPCC, 2007].

[3] Contrails form during the plume expansion phase when the mixture of hot, humid aircraft exhaust with colder ambient air surpasses saturation with respect to water, often at temperatures below  $-40^\circ\text{C}$ . Emitted soot and ultra-fine liquid aerosol particles initially act as cloud condensation nuclei prior to freezing to ice crystals. In the vortex phase, about 1 to 3 min behind the engine exit, mixing with ambient air is reduced. Ice crystals are captured within the descending vortex pair and adiabatic heating due to downward movement may lead to a partial sublimation of the ice crystals. Micrometer sized ice crystals with concentrations near  $1000 \text{ cm}^{-3}$  [Petzold et al., 1997; Schröder et al., 2000] and a few hundred  $\text{cm}^{-3}$  [Baumgardner and Gandrud, 1998] have been detected in 10 and 30 s old contrails from a Boeing B737 and a B757. In less than 180 s old contrails, ice crystals with effective radii  $r_{\text{eff}}$  of 1 to  $3 \text{ }\mu\text{m}$  and concentrations  $n_{\text{ice}}$  of several  $100 \text{ cm}^{-3}$  were reported [Schröder et al., 2000; Voigt et al., 2010].

[4] Further ice particle evolution and contrail to cirrus transition depends on vertical wind, relative humidity with respect to ice (RHI), wind shear, ambient temperature, and turbulence [Heymsfield et al., 2010]. Ice crystal  $r_{\text{eff}}$  up to  $5 \text{ }\mu\text{m}$  and concentrations below  $10 \text{ cm}^{-3}$  have been detected in up to 1 hour old contrails [Heymsfield et al., 1998; Schröder et al., 2000; Febvre et al., 2009]. A compilation of observations of contrail particle size and shape is given by Schumann et al. [2011]. Few measurements at visible wavelengths of the extinction and the optical depth of young contrails exist. Extinctions between  $0.3$  and  $0.5 \text{ km}^{-1}$  have been measured in sub-20 minute old contrails [Febvre et al., 2009] and optical depths of  $0.15$  to  $0.8$  have been reported for less than 1 hour old contrails [Gayet et al., 1996; Febvre et al., 2009].

[5] The overview of contrail measurements given above shows that, in particular, in situ observations of young contrails are sparse. In fact only 2 direct measurements of contrail ice crystal size distribution in the vortex phase exist [Baumgardner and Gandrud, 1998; Schröder et al., 2000] and potential instrumental shortcomings of the cloud probes preclude statements on the representativeness of these data. Further, there is no information on ice crystal shape or optical properties of contrails with ages of less than 2 min. Still, the vortex phase sets the stage for further contrail evolution hence is important for contrail model initialization and validation.

[6] Here we report results from extensive in situ measurements of young contrails in the vortex regime. The data were obtained during the CONCERT campaign - CONtrail and Cirrus ExpeRimenT - in November 2008 above Germany with instruments onboard the DLR research aircraft Falcon [Voigt et al., 2010]. More than 14 contrails from 9 different commercial aircraft were detected. We derive the size dis-

<sup>1</sup>Institut für Physik der Atmosphäre, Deutsches Zentrum für Luft- und Raumfahrt, Oberpfaffenhofen, Germany.

<sup>2</sup>Institut für Physik der Atmosphäre, Johannes-Gutenberg University, Mainz, Germany.

<sup>3</sup>LaMP, University Blaise Pascal, Clermont-Ferrand, France.

<sup>4</sup>IEK-7, Institute for Energy and Climate Research, Forschungszentrum Jülich, Jülich, Germany.

<sup>5</sup>Chemical Sciences Division, Earth System Research Laboratory, NOAA, Boulder, Colorado, USA.



**Figure 1.** Probing contrails from two A340 aircraft on 19 November 2008 above Germany, photo taken from the cockpit of the DLR-Falcon.

tribution, the ice water content (IWC) and probability density functions (PDF) of contrail extinction and optical depth typical for the present-day aircraft fleet and quantify related uncertainties. The measured contrail optical depth is used in radiative transfer calculations to estimate line-shaped contrail radiative forcing.

## 2. Particle Instrumentation

[7] We base our study on data obtained during the CONCERT campaign with the forward scattering spectrometer probe FSSP-300 mounted in the right wing station of the DLR research aircraft Falcon 20E [Petzold *et al.*, 1997; Schröder *et al.*, 2000; Voigt *et al.*, 2010]. In the instrument, the amount of light scattered by a single particle in forward directions is converted into particle size, which is resolved into an array of 31 channels. In the current study channels 30 and 31 are excluded because of instrumental noise and channels 10–14, 15–16, 17–18, 19–21, 22–23, 24–25, 26–29 are grouped according to ambiguities in the probe response

function derived from T-matrix calculations. Best agreement with the scattering phase function measured with a polar nephelometer [Gayet *et al.*, 1996] was achieved assuming aspherical particles with an aspect ratio of 0.5 composed of ice with a refractive index of 1.31.

## 3. Aircraft and Contrail Overview

[8] Fourteen contrails from nine different aircraft including an A380-841, a B767, an A340-642, an A340-311 (Figure 1), an A330-243, a B737-500, an A320, a CRJ-200 and an A319-111 were probed during the CONCERT campaign, whereby some of the contrails were repeatedly measured. Table 1 gives an overview of aircraft and contrail properties. The contrails were measured on 4 flights on 17 and 19 November 2008 at altitudes between 8.8 to 11.1 km and temperatures of 214 to 224 K. The contrails were identified from simultaneous increases in the NO mixing ratio above  $0.2 \text{ nmol mol}^{-1}$  detected with the NOy instrument [Voigt

**Table 1.** Overview of 14 Contrails From 9 Different Aircraft Detected on 17 and 19 November 2008 Over Germany<sup>a</sup>

Contrail Number	Aircraft Type	ff (Mg/h)	Weight (Mg)	FL	EI NO <sub>x</sub> (g kg <sup>-1</sup> )	T (K)	p (hPa)	RHI (%)	Age (s)
1	A340-311	2.1	240	300	18.5	224	309	84	61–145
2	B737-500	(1.2)	–	340	–	215	253	85	77–151
3	A340-642	2.5	342	310	16.6	218	262	90	82–139
4, 5, 7, 9	A319-111	1.2–0.9	47	350	11.2–8.7	220–218	240–250	80–89	63–184
6, 8	A340-311	1.3	150	350	11.6	217–218	243	75, 94	63–191
10, 11	B767	–	–	310	–	224	278	92, 96	66–135
12	CRJ-200	(0.5)	52	328	(9)	221	263	89	60–110
13	A380-841	(3.6)	508	350	(19.7)	217	244	93	66–266
14	A320	–	–	360	–	214	227	97	510–566

<sup>a</sup>Contrail number, aircraft type, fuel flow per engine (ff), weight, flight level (FL), NO<sub>x</sub> emission index (EI NO<sub>x</sub>), temperature (T), pressure (p), relative humidity with respect to ice (RHI) and contrail age are listed. Values in brackets are estimates.

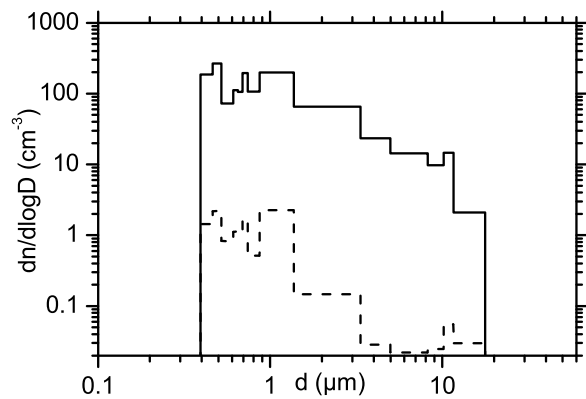


**Figure 2.** Contrail particle size distribution (solid line) for contrail ages between 55 and 566 s in the size range between 0.39 and 17.7  $\mu\text{m}$  averaged over 14 contrail encounters from 9 different aircraft. The lower tail of a cirrus distribution (dashed line) detected in the same size range under similar conditions for 1000 s prior to the encounter of the A380 contrail is shown for reference.

et al., 2006] and the concentration of cloud particles ( $d > 3 \mu\text{m}$ )  $> 0 \text{ cm}^{-3}$ . The contrail age was derived from the distance of the contrail-producing aircraft and the Falcon taking into account the contrail drift with the wind speed and direction measured by the Falcon. The contrails were observed at 9 to 160 km distance to the contrail-producing aircraft, corresponding to contrail ages of 55 to 566 s. The contrail sampling strategy is described in detail by Voigt et al. [2010].

[9] The mean RHI detected within contrails with the Lyman- $\alpha$  hygrometer FISH [Schiller et al., 2008; Kübbeler et al., 2010] was  $89 (\pm 11) \%$ . The frost point sensor (CR2) onboard the Falcon [Voigt et al., 2010] also measured on average  $89 (\pm 12) \%$  RHI. In each contrail the mean RHI ranged between 81 and 96% and one contrail (A340-311) was detected at 75% RHI. In the vortex phase, the dynamics are largely influenced by the downward motion of the vortex pair and adiabatic warming can explain subsaturation in contrails. In addition, inmixing of ice subsaturated ambient air might contribute to the observed in-contrail ice subsaturation. Six of the contrails were detected in clear sky (with particle number densities  $< 0.001 \text{ cm}^{-3}$  derived from FSSP data with  $d > 3 \mu\text{m}$ ), while 8 contrails were detected within optically thin natural cirrus clouds.

#### 4. Size Distribution, IWC, Extinction and Optical Depth of Contrails

[10] Figure 2 shows the mean particle size distribution from 14 contrail samplings using 2756 s of FSSP-300 data. Also shown for reference is FSSP particle size distribution detected in an optically thin cirrus cloud on 19 November 2008 immediately prior to entering the contrail from the A380 to investigate the effect of particle shattering on protruding probe inlets. The cirrus cloud contributes less than 1% to the number, surface and volume distribution detected in contrails, ruling out a significant interference from particle shattering. In addition, we observe no significant difference in the particle size range from 0.39 to 11.6  $\mu\text{m}$  between in-cirrus and out-of-cirrus contrail observations. Comparisons to particle size distributions measured in a 30 s old contrail from a B757 [Baumgardner and Gandrud, 1998] and to 1 and

5 min old contrails from an A300 and a B373 [Schröder et al., 2000], suggest these data are not significantly disturbed by instrumental artifacts either.

[11] We calculate the effective radius,  $r_{\text{eff}}$ , from the particle size distribution using  $r_{\text{eff}} = (3/4) V/A$ , where  $V$  is the total particle volume and  $A$  is the total projected particle cross-section [Schumann et al., 2011].  $r_{\text{eff}}$  is 2.9  $\mu\text{m}$  for the mean contrail size distribution, with 50% of the individual  $r_{\text{eff}}$  ranging between 2.1 and 3.8  $\mu\text{m}$ . Number densities in the  $0.39 < d < 17.7 \mu\text{m}$  size range are between 0.2 and  $578 \text{ cm}^{-3}$  with an average of  $117 \text{ cm}^{-3}$  for 1 to 10 min old contrails.

[12] In addition, we derive the ice water content from the FSSP volume distribution (Figure 3), the positive standard deviation is also shown. There is no clear temperature trend detectable at conditions near and below ice saturation. The mean IWC of  $2 \text{ mg m}^{-3}$  (8 ppmv, equivalent to 10% RHI) in the temperature range 214 to 224 K agrees with a parametrization by Schumann [2002]. The IWC parametrization by Heymsfield et al. [2010] for ambient RHI of 100.1% and 140% bound the CONCERT observations although the contrails were observed at a mean RHI of  $89 \pm 12\%$ . Further, we investigate the contribution of water produced by kerosene burning in the engines to the contrail IWC. Assuming similar dilution of  $\text{NO}_x$  and water vapor emissions, we derive the maximum  $\text{H}_2\text{O}$  engine contribution to the contrail IWC by multiplying the ratio of the  $\text{H}_2\text{O}$  (1230 g/kg) and the  $\text{NO}_x$  (13 g/kg) emission index with the measured  $\text{NO}_x$  mixing ratio taking into account the different molecular weights of the two species. On average, the engines contribute a significant amount of  $0.36 \text{ mg m}^{-3}$  (1.4 ppmv or  $\sim 18\%$ ) to our contrail IWC.

[13] We calculate the extinction coefficient from the integral over the projected particle cross section multiplied with the size dependent extinction efficiency at visible wavelengths (550 nm). A mean (median) extinction of 1.2 (0.7)  $\text{km}^{-1}$  shown in Figure 4 has been measured in the contrails. The extinction derived from the FSSP agrees well with the mean extinction of 1.2 (median 0.9)  $\text{km}^{-1}$  detected with the polar nephelometer [Gayet et al., 1996]. Differences may be related to different instrument sensitivities for small or large particles. The vertical

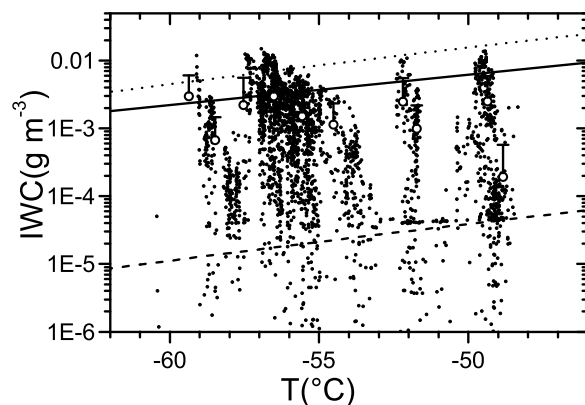


**Figure 3.** Temperature dependence of the ice water content of 14 young contrails from 9 different aircraft detected at  $89 \pm 12\%$  RHI. Open dots are 1 K bin means, error bars indicate one standard deviation in plus direction. The contrail IWC calculated from Schumann, 2002 (solid line), and Heymsfield et al. [2010] for RHI of 100.1% (dashed line) and 140% (dotted line) are shown for reference.

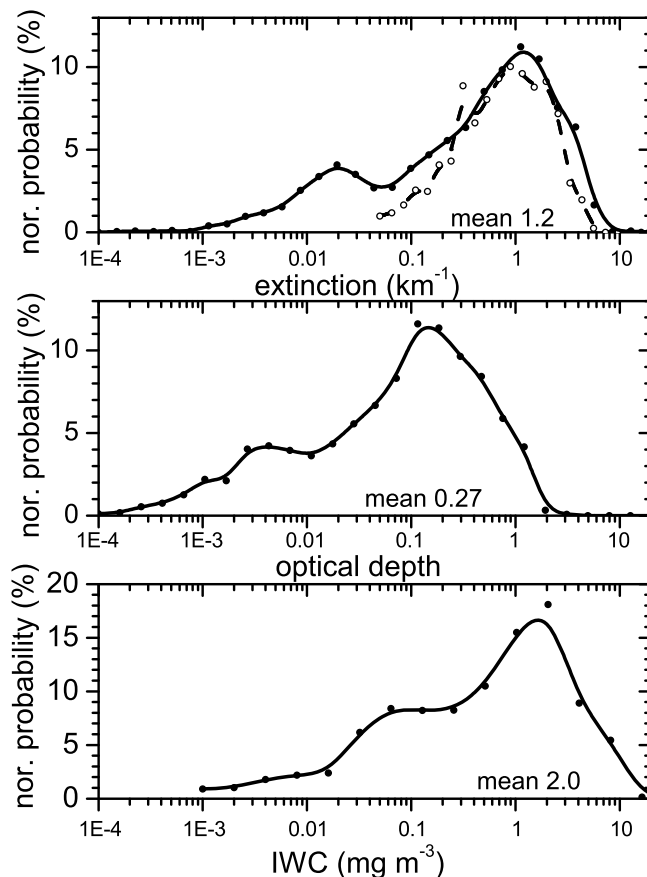


**Figure 4.** Normalized probability distributions of the extinction measured with the FSSP (solid circles) and the polar nephelometer (open circles), the optical depth and the ice water content from 2756 s of observations of 14 contrails from 9 different aircraft. A B-Spline is fitted to the data.

contrail depth for the individual aircraft has been calculated using dynamic vortex simulations by Holzäpfel [2006]. Typical values are 290 m for the A380, 210 m for the A340-300 and 120 m for the A319. The calculated contrail depths have in 3 cases been compared to the observations and agree within  $\pm 20\%$ .

[14] By multiplying the extinction with the calculated contrail depth we derive contrail optical depth  $\tau$ . The normalized probability distribution of  $\tau$  for the observed aircraft fleet is shown in Figure 4. The  $\tau$  distribution has a mean (median) of 0.27 (0.13). Increasing the lower  $\tau$  limit from 0.0001 to 0.01 leads to a mean (median)  $\tau$  of 0.32 (0.18). A further increase in the detection threshold to 0.05 results in a mean  $\tau$  of 0.41 (0.25).  $\tau$  of 0.15 and 0.25 have been derived in two 10 and 20 min old Embraer-170 contrails [Febvre *et al.*, 2009] and  $\tau$  of 0.8 has been measured in a less than an hour old contrail [Gayet *et al.*, 1996].

## 5. Radiative Forcing From Line-Shaped Contrails

[15] One of the large uncertainties in the estimate of line-shaped contrail radiative forcing (CRF) is their optical depth. Year-2000 CRF calculations summarized by IPCC [2007] yield a mean CRF of  $10 \text{ mWm}^{-2}$  (range  $6\text{--}15 \text{ mWm}^{-2}$ ).

The upper limit of  $15 \text{ mWm}^{-2}$  [Myhre and Stordal, 2001] has been derived for a fixed  $\tau$  of 0.3. The lower limit CRF of  $6 \text{ mWm}^{-2}$  [Marquart *et al.*, 2003] has been revisited recently and corrected to  $20 \text{ mWm}^{-2}$  caused by a calibration error, increased  $\tau$  (mean 0.13) and the trend in airtraffic [Kärcher *et al.*, 2010]. Sensitivity studies of CRF are given by Frömming *et al.* [2011].

[16] Here we use the mean  $\tau$  derived from an extensive in-situ dataset of contrail observations to estimate the radiative impact from linear persistent contrails. Under the assumption that the mean contrail  $\tau$  measured above western Europe under certain meteorological conditions was globally representative and that CRF is roughly proportional to  $\tau$  for low  $\tau$  [IPCC, 2007], we scale Myhre and Stordal's [2001] CRF linearly to our observed  $\tau$  of 0.27. This results in a year-2000 CRF of  $13.5 \text{ mWm}^{-2}$ . An 18% increase in CRF within the years 2000 to 2005 [Lee *et al.*, 2009] then leads to a year-2005 CRF of  $15.9 \text{ mWm}^{-2}$ .

[17] We now discuss the uncertainties in our estimated CRF. Instrumental uncertainties of  $\pm 30\%$  in the FSSP-300 data can linearly be converted into a CRF range. The  $\tau$  has been measured in slightly ice subsaturated air (mean RHI  $89 \pm 12\%$ ). Contrail formation at higher ice supersaturation will result in larger ice crystal surface areas and contrail optical depths. Further, the observed contrails had ages of less than 10 min, hence the evolution of individual contrails will depend on ambient conditions, particularly on RHI, T and wind fields. Kärcher *et al.* [2009] calculate the distribution of contrail properties for a typical range of meteorological conditions. Averaged over 4-hour contrail evolution they derive a mean contrail optical depth of 0.2 (their case FULL), varying between 0.05 and 0.5 for cases related to low ( $\sim 5\%$ ) and high ( $\sim 25\%$ ) ice supersaturation. Here, we use a factor of 3 in CRF to include the effects of contrail evolution, higher mean RHI and instrumental uncertainties and determine the CRF range  $11.1\text{--}47.7 \text{ mWm}^{-2}$  for the year 2005 ( $9.5\text{--}40.5 \text{ mWm}^{-2}$  for 2000).

## 6. Discussion and Outlook

[18] Extensive in-situ measurements of young contrails performed during the CONCERT campaign 2008 build the base for a robust investigation of microphysical and optical contrail properties such as particle size distribution, IWC, extinction and optical depth and their variability. Our observations extend the limited existing contrail data set to a wide range of aircraft types and to low ice saturation ratios. For the first time we present shape information for ice crystals in young contrails. Unlike previous assumptions, the scattering phase function suggests the dominance of aspherical particles in young contrails. Further investigations of the evolution of particle shape in ageing contrails are required.

[19] We probed 7 contrails from heavy aircraft (weight  $150\text{--}508 \text{ t}$ ) and 7 contrails from lighter aircraft ( $\sim 50 \text{ t}$ ). Although this aircraft statistics is naturally limited, we may speculate that our measured aircraft likely represent the present-day aircraft fleet. Under the assumption that the experimentally derived mean  $\tau$  of 0.27 was globally representative, the year-2000 linear contrail radiative forcing of  $13.5 \text{ mWm}^{-2}$  confirms the previous mean estimate of  $10 \text{ mWm}^{-2}$  [IPCC, 2007] with a tendency towards higher values. Our year-2005 CRF of  $15.9 \text{ mWm}^{-2}$  is within the range but on the high side of the CRF estimate of  $11.8 \text{ mWm}^{-2}$  by Lee *et al.* [2009]. Given

the above mentioned uncertainties, further measurements and global model simulations are required to better constrain the radiative forcing from contrails in a present and future climate.

[20] **Acknowledgments.** The CONCERT campaign was organized by the HGF-junior research group AEROTROP (<http://www.pa.op.dlr.de/AEROTROP>). Part of this work was funded within the DLR-project CATS and by the DFG SPP HALO 1294. We thank the DLR flight department, the Deutsche Lufthansa (A. Waibel) and DFS for excellent support. D. Schäuble, T. Hamburger, A. Minikin and J. Gasteiger are thanked for instrument preparation. H. Schlager provided NO<sub>y</sub> data. We further thank M. Ponater, C. Frömming and R. Rodríguez de Leon for stimulating discussions.

[21] The Editor thanks the two anonymous reviewers for their assistance in evaluating this paper.

## References

- Baumgardner, D., and B. E. Gandrud (1998), A comparison of the microphysical and optical properties of particles in an aircraft contrail and mountain wave cloud, *Geophys. Res. Lett.*, **25**, 1129–1132, doi:10.1029/98GL00035.
- Febvre, G., J.-F. Gayet, A. Minikin, H. Schlager, V. Shcherbakov, O. Jourdan, R. Busen, M. Fiebig, B. Kärcher, and U. Schumann (2009), On optical and microphysical characteristics of contrails and cirrus, *J. Geophys. Res.*, **114**, D02204, doi:10.1029/2008JD010184.
- Frömming, C., et al. (2011), Sensitivity of contrail coverage and contrail radiative forcing to selected key parameters, *Atmos. Environ.*, **45**, 1483–1490.
- Gayet, J.-F., et al. (1996), Microphysical and optical properties of cirrus and contrails, *J. Atmos. Sci.*, **53**, 126–138.
- Heymsfield, A. J., R. P. Lawson, and G. W. Sachse (1998), Growth of ice crystals in a precipitating contrail, *Geophys. Res. Lett.*, **25**, 1335–1338.
- Heymsfield, A., et al. (2010), Contrail microphysics, *Bull. Am. Meteorol. Soc.*, **91**, 465–471.
- Holzäpfel, F. (2006), Probabilistic two-phase aircraft wake-vortex model: Further development and assessment, *J. Aircr.*, **43**, 700–708.
- Intergovernmental Panel on Climate Change (IPCC) (2007), *Climate Change 2007: The Physical Science Basis. Contribution of Working Group I to the Fourth Assessment Report of the Intergovernmental Panel on Climate Change*, edited by S. Solomon et al., Cambridge Univ. Press, Cambridge, U. K.
- Kärcher, B., U. Burkhardt, S. Unterstrasser, and P. Minnis (2009), Factors controlling contrail cirrus optical depth, *Atmos. Chem. Phys.*, **9**, 6229–6254.
- Kärcher, B., U. Burkhardt, M. Ponater, and C. Frömming (2010), Importance of representing optical depth variability for estimates of global line-shaped contrail radiative forcing, *Proc. Natl. Acad. Sci. U. S. A.*, **107**, 19,181–19,184, doi:10.1073/pnas.1005555107.
- Kübbeler, M., et al. (2010), Thin and subvisible cirrus and contrails in a sub-saturated environment, *Atmos. Chem. Phys. Discuss.*, **10**, 31,153–31,186, doi:10.5194/acpd-10-31153-2010.
- Lee, D. S., et al. (2009), Aviation and global climate change in the 21st century, *Atmos. Environ.*, **43**, 3520–3537, doi:10.1016/j.atmosenv.2009.04.024.
- Marquart, S., M. Ponater, F. Mager, and R. Sausen (2003), Future development of contrail cover, optical depth, and radiative forcing: Impacts of increasing air traffic and climate change, *J. Clim.*, **16**, 2890–2904.
- Myhre, G., and F. Stordal (2001), On the tradeoff of the solar and thermal infrared radiative impact of contrails, *Geophys. Res. Lett.*, **28**, 3119–3122.
- Petzold, A., et al. (1997), Near-field measurements on contrail properties from fuels with different sulfur content, *J. Geophys. Res.*, **102**, 29,867–29,880.
- Schiller, C., M. Krämer, A. Afchine, N. Spelten, and N. Sitnikov (2008), Ice water content of Arctic, midlatitude, and tropical cirrus, *J. Geophys. Res.*, **113**, D24208, doi:10.1029/2008JD010342.
- Schröder, F., et al. (2000), On the transition of contrails into cirrus clouds, *J. Atmos. Sci.*, **57**, 464–480.
- Schumann, U. (2002), Contrail cirrus, in *Cirrus*, edited by D. K. Lynch et al., pp. 231–255, Oxford Univ. Press, New York.
- Schumann, U., et al. (2011), Effective radius of ice particles in cirrus and contrails, *J. Atmos. Sci.*, **68**, 300–321, doi:10.1175/2010JAS3562.1.
- Voigt, C., et al. (2006), Nitric acid in cirrus clouds, *Geophys. Res. Lett.*, **33**, L05803, doi:10.1029/2005GL025159.
- Voigt, C., et al. (2010), In-situ observations of young contrails—Overview and selected case studies from the CONCERT campaign, *Atmos. Chem. Phys.*, **10**, 9039–9056, doi:10.5194/acp-10-9039-2010.
- D. W. Fahey and T. Thornberry, Chemical Sciences Division, Earth System Research Laboratory, NOAA, 325 Broadway, Boulder, CO 80305, USA.
- J.-F. Gayet, LaMP, University Blaise Pascal, 24, Avenue des Landais, F-63177 Clermont-Ferrand CEDEX, France.
- P. Jessberger, T. Jurkat, A. Petzold, U. Schumann, and C. Voigt, Institut für Physik der Atmosphäre, Deutsches Zentrum für Luft- und Raumfahrt, Postfach 1116, D-82234 Oberpfaffenhofen, Germany. ([christiane.voigt@dlr.de](mailto:christiane.voigt@dlr.de))
- M. Krämer, IEK-7, Institute for Energy and Climate Research, Forschungszentrum Jülich, D-52425 Jülich, Germany.